STUDY OF DOS (DENSITY OF STATE) OF HALIDE PEROVSKITES $CH_3NH_3PbI_3$ USING TROTTER-SUZUKI TIME PROPAGATION METHOD

Teguh Iman Perdana*, Sholihun, Iman Santoso
Department of Physics, Faculty of Mathematics and Natural Sciences, Universitas Gadjah Mada, Sekip Utara, Yogyakarya, 55281, Indonesia
*email: teguh.i@mail.ugm.ac.id

ABSTRACT

This study investigates the electronic properties of $CH_3NH_3PbI_3$ using the tight-binding time propagation method (TB-TPM) combined with the Trotter-Suzuki decomposition. The research focuses on computing the density of states (DOS) for various system sizes and time step parameters, employing a real-space approach to model the electronic structures of the material. Considering only the s-orbitals of Pb and I atoms reduces the computational complexity, enabling efficient simulations. The results indicate a metallic behavior, deviating from the expected semiconducting properties reported in prior studies due to the exclusion of critical p-orbital interactions. The study also highlights the effect of timestep size on the accuracy of the correlation functions and DOS, emphasizing the need for smaller timesteps to resolve spectral features effectively.

Keywords: *$CH_3NH_3PbI_3$; Tight-binding; Density of states; Trotter-Suzuki; Electronic structure*

INTRODUCTION

The rapid advancements in renewable energy technologies have significantly increased the demand for efficient and cost-effective materials for solar energy conversion. Among these, hybrid organic-inorganic perovskites, particularly methylammonium lead iodide ($CH_3NH_3PbI_3$), have garnered substantial attention due to their exceptional optoelectronic properties (Wang *et al*, 2020). These properties include high absorption coefficients (Kovalenko *et al*, 2017), long carrier diffusion lengths (Shi *et al*, 2015), and tunable bandgaps (Noh *et al*, 2013), making them promising candidates for next-generation photovoltaic devices (Kojima *et al*, 2009).

Despite their remarkable performance in solar cell applications, a comprehensive understanding of the electronic structure of $CH_3NH_3PbI_3$ remains essential to optimize their functionality further. The density of states (DOS), as a critical descriptor of the electronic structure, plays a pivotal role in determining its optical and electrical behavior (Bannow *et al*, 2019). Consequently, accurate computational methods are imperative for studying these properties and providing insights into the fundamental mechanisms governing the material performance (Brivio *et al*, 2013).

Traditionally, density functional theory (DFT) (Kresse & Furthmüller, 1996) and tight-binding models in k-space (Slater & Koster, 1954) have been the primary computational approaches used to investigate the electronic structure of perovskites. While these methods have provided valuable insights, they are not without limitations. DFT, for instance, can be computationally demanding and often requires approximations that may not fully capture the complex electronic interactions in hybrid perovskites (Perdew *et al*, 1996). On the other hand, tight-binding models in k-space, although computationally efficient, can sometimes lack the flexibility needed to describe certain features of disordered or real-space systems (S. Ashhab *et al*, 2017).

In this study, we employ the tight-binding propagation method to explore the density of states (DOS) of $CH_3NH_3PbI_3$. Unlike the conventional k-space tight-binding approach, the tight-binding propagation method operates in real space, offering a unique perspective on the electronic structure (Welborn *et al*, 2013). This approach is particularly advantageous for systems with structural complexities or disorders, as it inherently accounts for spatial variations in electronic interactions (Balagurov *et al*, 2004). In this study, we limit our calculation to the s-orbital of the lead (Pb) atoms in $CH_3NH_3PbI_3$. This choice is justified by the dominant contribution of the Pb s-orbital to the conduction band minimum (CBM) and its critical role in determining the electronic properties of the material. By focusing on the Pb s-orbital, we reduce the computational complexity while retaining the essential physics of the electronic structure. This simplification allows us to efficiently model the key

features of the DOS without compromising the accuracy of the results.

The calculation of the DOS in our approach involves the Fast Fourier Transform (FFT) of the correlation function, which requires solving the time-dependent Schrödinger equation (TDSE). A key component of this solution is applying the Trotter-Suzuki decomposition method (Suzuki, 1990). The Trotter-Suzuki method enables an efficient and accurate wavefunction propagation in time by splitting the Hamiltonian into manageable parts and systematically approximating the time evolution operator (Ariasoca, 2018). This methodology is crucial for capturing the dynamic evolution of the system and obtaining precise DOS results. By integrating the Trotter-Suzuki decomposition into the tight-binding propagation framework, we aim to provide a deeper understanding of the electronic structure of $CH_3NH_3PbI_3$ and highlight its implications for designing and optimizing high-performance solar cell devices.

This work demonstrates the applicability of the tight-binding propagation method, complemented by advanced techniques like the Trotter-Suzuki decomposition, to hybrid perovskites. It underscores its potential as a complementary tool to conventional computational methods. Through this study, we contribute to bridging the gap in the theoretical understanding of perovskite materials and pave the way for further advancements in their application to energy conversion technologies.

COMPUTATIONAL DETAILS

$CH_3NH_3PbI_3$ Structure

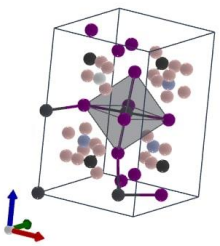

Figure 1 $CH_3NH_3PbI_3$ Structure. Grey represents the Pb atoms. Purple represents I atoms. Dark Grey represents the C atoms. Blue represents the N atom. Pink represents the H atom.

The structure used in this calculation is shown in Figure 1. The choice of cubic structure is for simplicity.

$CH_3NH_3PbI_3$ Hamiltonian Matrix

The Hamiltonian matrix for $CH_3NH_3PbI_3$ is constructed using the tight-binding model, incorporating contributions from the lead, iodine, and methylammonium ions. The general form of the Hamiltonian can be expressed as:

$$H = \sum_{i,j} -t_{i,j} c_i^{\dagger} c_j + \sum_i v_i c_i^{\dagger} c_i \qquad (1)$$

where $-t_{i,j}$ represents the hopping parameter between nearest-neighbor sites, v_i is the on-site potential of Pb (6s-orbital) and I (5s-orbital) atoms. For simplicity, the $CH_3NH_3PbI_3$ lattice is treated as a perovskite cubic lattice structure, with hopping and potential terms adjusted to reflect the electronic interactions specific to the perovskite material.

The Hamiltonian matrix for a $N \times N \times N$ cubic system will have a size of $N^3 \times N^3$. The matrix is constructed by mapping the hopping parameters and on-site potentials onto the lattice configuration. The matrix representation of this Hamiltonian will be:

$$H = H_X + H_Y + H_Z, \qquad (2)$$

with H_X, H_Y, H_Z represent the propagation interaction throughout the x,y,z directions, respectively. For a $5 \times 5 \times 5$ system, the matrix representation will be given by

$$H_x = \begin{bmatrix} A & B & A & B & A \\ B & C & B & C & B \\ A & B & A & B & A \\ B & C & B & C & B \\ A & B & A & B & A \end{bmatrix} \qquad (3)$$

where

$$A = \begin{bmatrix} 0 & 0 & 0 & 0 & 0 \\ 0 & 0 & 0 & 0 & 0 \\ 0 & 0 & 0 & 0 & 0 \\ 0 & 0 & 0 & 0 & 0 \\ 0 & 0 & 0 & 0 & 0 \end{bmatrix} \qquad (4)$$

$$B = \begin{bmatrix} 0 & 0 & 0 & 0 & 0 \\ 0 & v_I & 0 & -t & 0 \\ 0 & 0 & 0 & 0 & 0 \\ 0 & -t & 0 & v_I & 0 \\ 0 & 0 & 0 & 0 & 0 \end{bmatrix} \qquad (5)$$

$$C = \begin{bmatrix} v_I & -t & 0 & 0 & -t \\ -t & v_{Pb} & -t & 0 & 0 \\ 0 & -t & v_I & -t & 0 \\ 0 & 0 & -t & v_{Pb} & -t \\ -t & 0 & 0 & -t & v_I \end{bmatrix} \qquad (6)$$

for the interaction in x-direction. As for interaction in the y and z direction, the matrix representations H_y, H_z will be the same, but they only differ in the index of the atom (atomic positions).

2.2. Trotter-Suzuki Product Formula

To solve the time-dependent Schrödinger equation (TDSE) for $CH_3NH_3PbI_3$, we employ the Trotter-Suzuki product formula. This method decomposes the Hamiltonian into manageable sub-operators that are easier to exponentiate. The first-order Trotter-Suzuki approximation is given by:

$$U(\tau) \approx e^{-i\tau H_1} e^{-i\tau H_2} \dots e^{-i\tau H_n}, \quad (7)$$

where H_i is the decomposed components of the Hamiltonian, and τ is the discrete time step. This decomposition significantly reduces the computational complexity associated with the time evolution operator.

Each exponential term in the Trotter-Suzuki product is calculated using a Taylor expansion:

$$e^X = I + X + \frac{X \cdot X}{2!} + \frac{X \cdot X \cdot X}{3!} + \dots \quad (8)$$

For $CH_3NH_3PbI_3$, the Hamiltonian matrix is partitioned into block matrices corresponding to the lead, iodine, and methylammonium sub-lattices. These blocks are then exponentiated individually, ensuring that the structural and electronic properties unique to the perovskite are preserved.

The initial states are represented by random complex numbers within the range $(-1, 1)$ at each site.

Consequently, the wavefunction of the system is expressed as a linear combination:

$$|\psi_0\rangle = \sum_{\alpha} a_\alpha \psi_\alpha \ , a_\alpha \in \mathbb{C}, \quad (9)$$

where a_α denotes the expansion coefficients. TDSE is then solved for this initial state to compute the correlation function:

$$C(\tau) = \langle \psi_0 | e^{-i\tau H} | \psi_0 \rangle \quad (10)$$

This process is repeated for each discrete time step over N iterations. Finally, the DOS is obtained by applying the Fourier transform to the inner product of the wavefunction:

$$D(E) = \lim_{s\to\infty} \frac{1}{S} \sum_{p=1}^{S} \frac{1}{2\pi} \int_{-\infty}^{\infty} e^{itE} \langle \psi_0 | e^{-itH} | \psi_0 \rangle \, dt \quad (11)$$

This method ensures an accurate representation of the DOS while maintaining computational efficiency for large systems.

RESULTS AND DISCUSSIONS

The calculated correlation functions and DOS for the $CH_3NH_3PbI_3$ using Trotter-Suzuki TB-TPM across different sizes (5×5×5, 15×15×15, and 25×25×25) are shown in Figure 1(a), (c), (e) and 1(b), (d), (f), respectively, exhibit metallic behavior, as indicated by the absence of a band gap at the Fermi level in the DOS. This result deviates significantly from the semiconducting nature typically reported for perovskites.

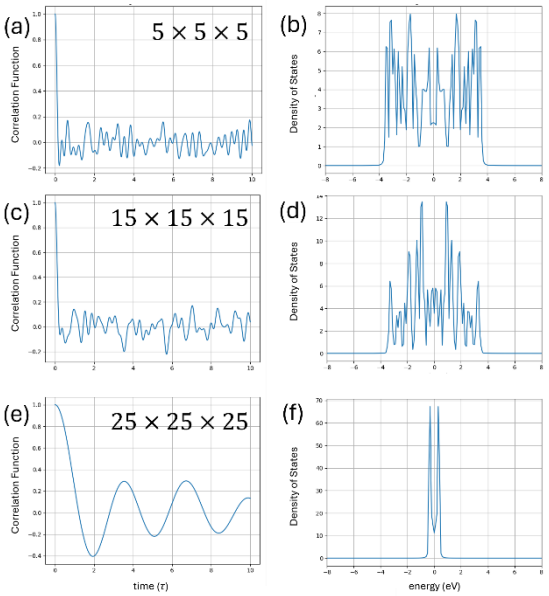

Figure 2 Correlation Function for (a) $5 \times 5 \times 5$, (c) $15 \times 15 \times 15$, (e) $25 \times 25 \times 25$ and Density of States for (b) $5 \times 5 \times 5$, (d) $15 \times 15 \times 15$, (f) $25 \times 25 \times 25$ using time steps $\tau = 0.1$ with $t = -1.2\ eV$ and $v_{Pb} = v_{Pb} = 1.5\ eV$.

In prior DFT calculations (Umari *et al*, 2021) and k-space tight-binding models (Boyer-Richard *et al*, 2016). the electronic structure of perovskites is dominated by hybridization between the Pb 6p orbitals (conduction band minimum) and the I 5p orbitals (valence band maximum). These studies consistently reveal a finite band gap characteristic of semiconducting behavior. In contrast, our tight-binding calculation considers only the 6s orbital of Pb and the 5s orbital of I. This simplification excludes the key p-orbitals essential for forming the valence and conduction bands, resulting in overlapping s-orbital bands and a continuous DOS, producing an artificial metallic behavior.

Moreover, the broad and overlapping 6s-orbital bands lack the resolution needed to replicate the distinct states near the Fermi level observed in

DFT and k-space tight-binding calculations. The absence of p-orbital interactions eliminates the hybridization effects necessary to open a band gap (Goesten & Hoffmann, 2018), underscoring the limitations of the current tight-binding model.

Regarding correlation functions, the results show increased coherence and oscillatory behavior for larger system sizes. Still, these do not capture the actual semiconducting properties due to omitting 6p-orbital contributions of Pb and 5p-orbital of I atoms.

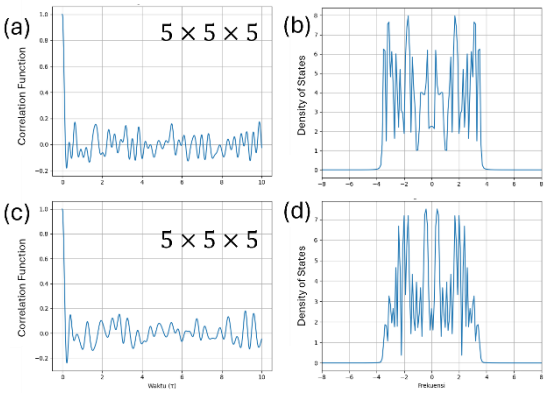

Figure 3 Correlation Function for $5 \times 5 \times 5$ using time steps (a) $\tau = 0.1$, (c) $\tau = 0.01$ and Density of States for (b) $\tau = 0.1$, (d) $\tau = 0.01$ with $t = -1.2\ eV$ and $v_{Pb} = v_{Pb} = 1.5\ eV$.

Figure 3 shows the correlation function and density of states (DOS) calculation time steps using $\tau = 0.1$ and $\tau = 0.01$ to show the impact of timestep size on the results. The correlation function exhibits an initial rapid decay in the oscillation behavior. These oscillations are smoother and better resolved for $\tau = 0.01$ compared to $\tau = 0.1$, indicating improved numerical accuracy with smaller timesteps.

The DOS shows distinct peaks characteristic of a tight-binding band structure. For $\tau = 0.01$, the peaks are sharper and more defined, while $\tau = 0.1$ introduces numerical artifacts that obscure spectral details. This result highlights the importance of using smaller timesteps for accurately resolving spectral features via the Fourier transform.

CONCLUSION

In summary, we performed tight-binding time propagation using the Trotter-Suzuki method to calculate the density of states (DOS) for $CH_3NH_3PbI_3$ across various system sizes and time step parameters. This approach offers computational efficiency by circumventing the diagonalization of the Hamiltonian matrix, a process that becomes increasingly demanding for larger systems. Our findings indicate that $CH_3NH_3PbI_3$ exhibits metallic behavior, which contrasts with previous experimental results and calculations. This discrepancy arises from our model's use of s-orbitals instead of p-orbitals for Pb and I atoms. For a more comprehensive depiction of the material's electronic properties, future work should incorporate p-orbital interactions and spin-orbit coupling.

Our model emphasizes the contribution of Pb atoms to the electronic structure, given their significant role in defining the conduction and valence band edges of $CH_3NH_3PbI_3$. While elements such as iodine and the organic cation $CH_3NH_3^+$ also influence the electronic properties, their effects are considered secondary and can be integrated into future model refinements. This simplification aligns with previous studies on lead halide perovskites, which underscore the central role of Pb orbitals in electronic characteristics. For instance, it has been demonstrated that a tight-binding model focusing on Pb orbitals effectively captures the band structure of inorganic lead halide perovskites (Nestoklon, 2020). Additionally, density functional theory also used to analyze $CH_3NH_3PbI_3$, highlighting the dominance of Pb and I orbitals in the electronic structure (Wang *et al.*, 2014). Incorporating insights from such studies will enhance the robustness of tight-binding analyses and support their broader applicability across hybrid materials.

REFERENCES

Ariasoca, T. A., Sholihun, & Santoso, I. (2019). Trotter-Suzuki-time propagation method for calculating the density of states of disordered graphene. *Computational Materials Science*, *156*, 434–440. https://doi.org/10.1016/j.commatsci.2018.10.016

Balagurov, D. B., Malyshev, V. A., & Domínguez Adame, F. (2004). Phase coherence in tight-binding models with nonrandom long-range hopping. *Physical Review B*, *69*(10). https://doi.org/10.1103/physrevb.69.104204

Bannow, L. C., Hader, J., Moloney, J. V., & Koch, S. W. (2019). Microscopic calculation of the optical properties and intrinsic losses in the methylammonium lead iodide perovskite system. *APL Materials*, 7(1), 011107. https://doi.org/10.1063/1.5078791

Boyer-Richard, S., Katan, C., Traoré, B., Scholz, R., Jancu, J.-M., & Even, J. (2016). Symmetry-Based Tight Binding Modeling of Halide Perovskite Semiconductors. *The Journal of Physical Chemistry Letters*, *7*(19), 3833–3840. https://doi.org/10.1021/acs.jpclett.6b01749

Brivio, F., Walker, A. B., & Walsh, A. (2013). Structural and electronic properties of hybrid perovskites for high-efficiency thin-film photovoltaics from first-principles. *APL Materials*, *1*(4), 042111. https://doi.org/10.1063/1.4824147

Goesten, M. G., & Hoffmann, R. (2018). Mirrors of Bonding in Metal Halide Perovskites. *Journal of the American Chemical Society*, *140*(40), 12996–13010. https://doi.org/10.1021/jacs.8b08038

Kojima, A., Teshima, K., Shirai, Y., & Miyasaka, T. (2009). Organometal Halide Perovskites as Visible-Light Sensitizers for Photovoltaic Cells. *Journal of the American Chemical Society*, *131*(17), 6050–6051. https://doi.org/10.1021/ja809598r

Kovalenko, M. V., Protesescu, L., & Bodnarchuk, M. I. (2017). Properties and potential optoelectronic applications of lead halide perovskite nanocrystals. *Science*, *358*(6364), 745–750. https://doi.org/10.1126/science.aam7093

Kresse, G., & Furthmüller, J. (1996). Efficient iterative schemes forab initiototal-energy calculations using a plane-wave basis set. *Physical Review B*, *54*(16), 11169–11186. https://doi.org/10.1103/physrevb.54.11169

Nestoklon, M. O. (2020). Tight-binding description of inorganic lead halide perovskites in cubic phase. *arXiv preprint arXiv:2012.14705*.

Noh, J. H., Im, S. H., Heo, J. H., Mandal, T. N., & Seok, S. I. (2013). Chemical Management for Colorful, Efficient, and Stable Inorganic–Organic Hybrid Nanostructured Solar Cells. *Nano Letters*, *13*(4), 1764–1769. https://doi.org/10.1021/nl400349b

Paolo Umari, Mosconi, E., & Angelis, F. D. (2021). *Relativistic GW calculations on CH3NH3PbI3 and CH3NH3SnI3 perovskites for solar cell applications*. Unboundmedicine.com. https://www.unboundmedicine.com/medline/citation/24667758/Relativistic_GW_calculations_on_CH3NH3PbI3_and_CH3NH3SnI3_perovskites_for_solar_cell_applications_

Perdew, J. P., Burke, K., & Ernzerhof, M. (1996). Generalized Gradient Approximation Made Simple. *Phys. Rev. Lett.*, *77*(18), 3865–3868. https://doi.org/10.1103/physrevlett.77.3865

S. Ashhab, O. Voznyy, Hoogland, S., Sargent, E. H., & Madjet, M. E. (2017). Effect of disorder on transport properties in a tight-binding model for lead halide perovskites. *Scientific Reports*, *7*(1). https://doi.org/10.1038/s41598-017-09442-4

Shi, D., Adinolfi, V., Comin, R., Yuan, M., Alarousu, E., Buin, A., Chen, Y., Hoogland, S., Rothenberger, A., Katsiev, K., Losovyj, Y., Zhang, X., Dowben, P. A., Mohammed, O. F., Sargent, E. H., & Bakr, O. M. (2015). Low trap-state density and long carrier diffusion in organolead trihalide perovskite single crystals. *Science*, *347*(6221), 519–522. https://doi.org/10.1126/science.aaa2725

Slater, J. C., & Koster, G. F. (1954). Simplified LCAO Method for the Periodic Potential Problem. *Physical Review*, *94*(6), 1498–1524. https://doi.org/10.1103/physrev.94.1498

Suzuki, M. (1990). Fractal decomposition of exponential operators with applications to many-body theories and Monte Carlo simulations. *Physics Letters A*, *146*(6), 319–323. https://doi.org/10.1016/0375-9601(90)90962-n

Wang, H., Wang, X., Zhang, H., Ma, W., Wang, L., & Zong, X. (2020). Organic−inorganic hybrid perovskites: Game-changing candidates for solar fuel production. *Nano Energy*, *71*, 104647. https://doi.org/10.1016/j.nanoen.2020.104647

Wang, Y., Gould, T., Dobson, J. F., Zhang, H., Yang, H., Yao, X., & Zhao, H. (2014). Density functional theory analysis of structural and electronic properties of orthorhombic perovskite $CH_3NH_3PbI_3$. *Physical Chemistry Chemical Physics*, 16(4), 1424-1429.

Welborn, M., Chen, J., & Van Voorhis, T. (2013). Densities of states for disordered systems from free probability. *Physical Review B*, *88*(20). https://doi.org/10.1103/physrevb.88.205113